APPENDIX A

CONDITION ASSESSMENT OF SIDE-BY-SIDE BOX BEAM BRIDGE CARRYING US-24 OVER MIDDLE ROUGE RIVER

By

Dr. Elin Jensen, Principal Investigator

Dr. Nabil Grace, Co-Principal Investigator

Department of Civil and Architectural Engineering

Lawrence Technological University

Southfield, MI 48075-0134

November 2015

A.0 Summary

The evaluation by Magnetic Flux Leakage Method indicated significant loss of cross section area of the lower layer prestressing strands in Beam 3. It is estimated that three (3) of thirteen (13) prestressing strands are fully corroded, and that five (5) of thirteen (13) are corroded about 15-75 %. The 3D ultrasonic tomography method also supports delamination around these same strands.

The lower layer prestressing strands in Box Beam 2 does not exhibit significant magnetic flux leakage. At the same time, no significant delamination is captured by the 3D ultrasonic tomography method.

A.1 Description

In November, 2014. MDOT approached the research team to conduct a field evaluation of the magnetic flux leakage and the 3D ultrasonic tomography methods; the primary non-destructive evaluation techniques evaluated in this study. The investigations were to assess the extent of cross-sectional area loss due to corrosion of the bottom strands using magnetic flux leakage method and also to assess un-exposed sections of the beams for initiation of delamination around strands using the 3D ultrasonic tomography method.

A.2 Bridge Details

The selected structure was a prestressed box beam bridge carrying north bound US-24 over the Middle Rouge River in Redford Township, Oakland County. The bridge is located about 0.4 miles south of Five Mile Road. During recent scheduled MDOT field inspection, some box beams were reported in poor condition with observed extensive spallings and rust leakage on the box beam bottom surfaces. The beams of primary concern were the three most western beams in the northern span of the north bound bridge. The deterioration extended from the northern abutment towards the mid span area. The outside northbound lane was closed to traffic as a precaution.

The Lawrence Technological University (LTU) research team conducted a site visit in late November to determine the site conditions, confirm the areas of extensive delamination, spallings, rust stains and determine the test area and associated layout for the testing protocols. A schematics of the bridge is shown in Figure 1. The work conducted by LTU was performed under the Permit Number: 97000-026443-071714. A copy of the permit is available at the end of this appendix under supplemental material.

The initial site visit and visual evaluation conducted by the LTU research team confirmed longitudinal cracking in the deck surface above the location of shear keys between the adjacent box beams, exposed corroded bottom strands on one of the beams, with other sections of the three beams under consideration showing extensive signs of delamination and spallings. The non-destructive assessment was to be focused on the three exterior box beams on the western side of the north bound bridge (Figure 2).

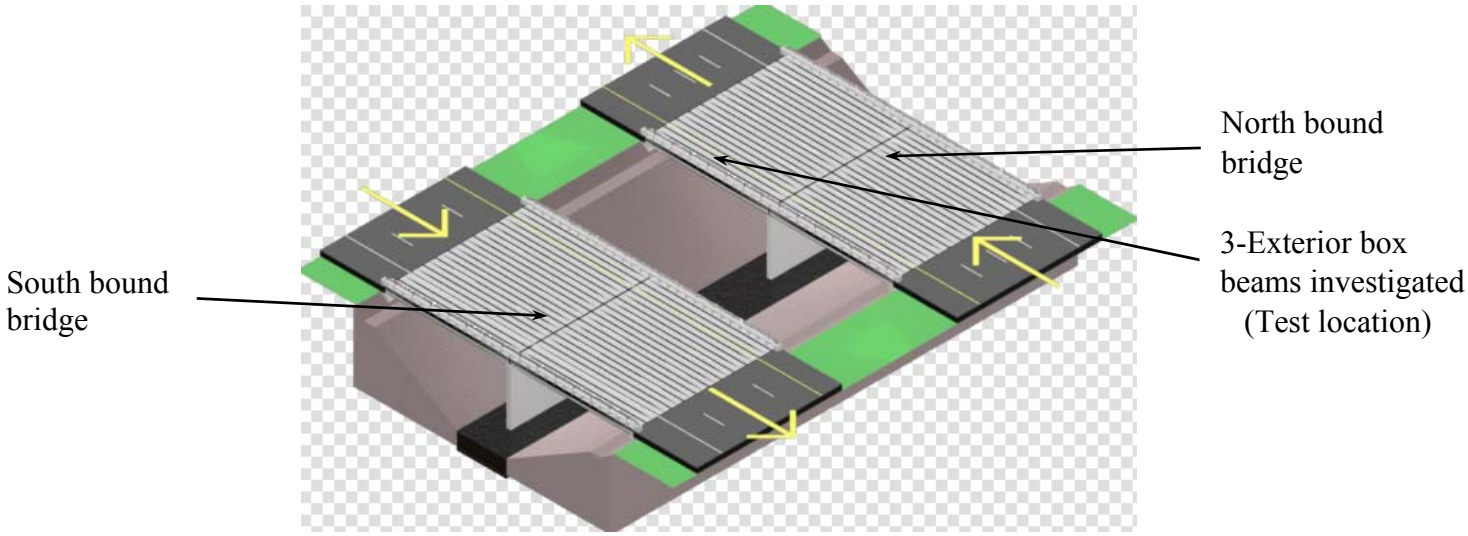

Figure 1: Overview of bridge showing test location. Center pier located in the Middle Rouge River.

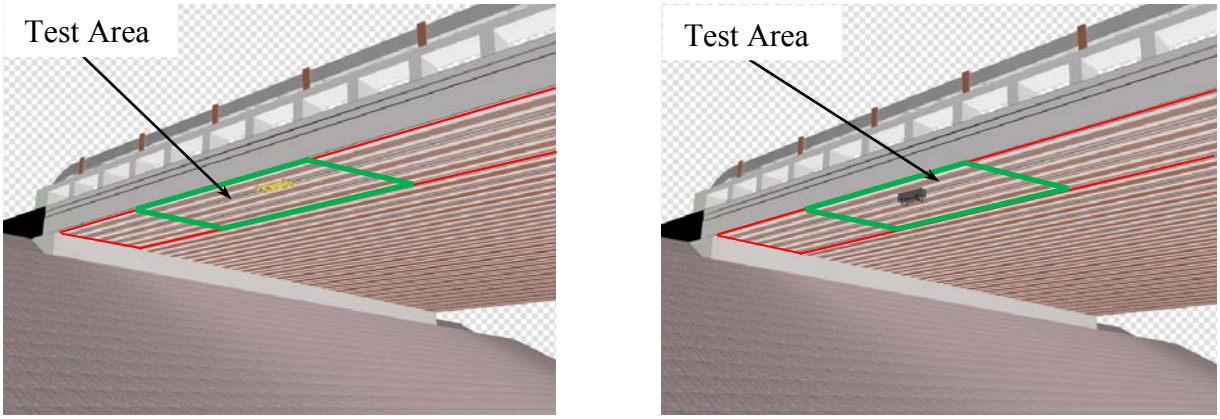

Figure 2: Overview of underside of bridge showing test location for MFL and 3D Tomography

The box beams had span length of 60'-4" spanning from the abutment on the north side to the center piers. Due to site constraints, only 9' of the span length was accessible starting 7' from the abutment towards the Middle Rouge River. The river was channeled under the bridge and the slope from the river bank to the northern abutment was paved with blocks on a slope of about 1 in 2. To aid the reach to the box beam bottom surfaces, a temporary mobile support system was constructed as shown in Figure 3.

Figure 3: Overview of Temporary Mobile Support

The field investigation was conducted from December 4, 2014 to December 11, 2014. Nondestructive evaluation of the three selected box beams were conducted using the magnetic flux leakage equipment developed and built by Lawrence Technological University to evaluate the extent of potential cross-sectional area loss. The magnetic flux leakage equipment was developed as part of the main research project (# JN 116238). The extent of hidden delamination around strands was also assessed using a 3D ultrasonic tomography method. Details and findings of the two nondestructive evaluation methods are outlined in this appendix. Examples of the deterioration is shown in Figures 4 and 5.

Fig. 4: Overview of underside of bridge

Fig. 5: Exposed tone strand of box beam

All tests were performed directly on the avaliable bottom surfaces of the selected box beams. The location of the bottom layer strands (3/8” 7 wire) of the two (2) most affected box beams designated as Beam 2 and 3 were mapped out.

Details of box beams were extracted from as-built drawings with designation Brighton-Detroit Road from Job Number 01247A DWG No. B03 of 82053C, Superstructure Details. The cross-section of the box beams as well as the designated numbers used for the botom strand layer for testing purpose are shown in Figures 6 and 7. The longitudinal section of the box beams indicating testing location from the north abutment have been shown in Figure 8. Beams designation and testing locations for strands 3 and 8 for beams 2 and 3 have been mapped out on Figure 9.

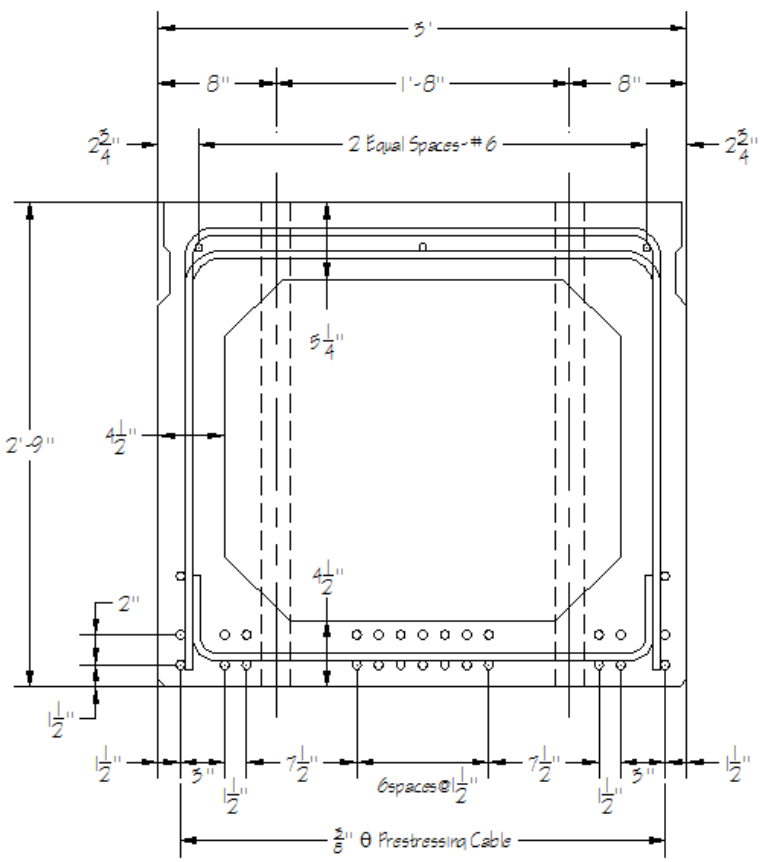

Figure 6: Typical Cross-section of Box Beams for US-24 with Doubled layered 3/8” strand at 2” vertical spacing and stirrup spacing of 18” (Adapted from State Project I-82122-035, Job No. 01247A, Sheet No. B03 of 82053C and B1 of 82-16-1)

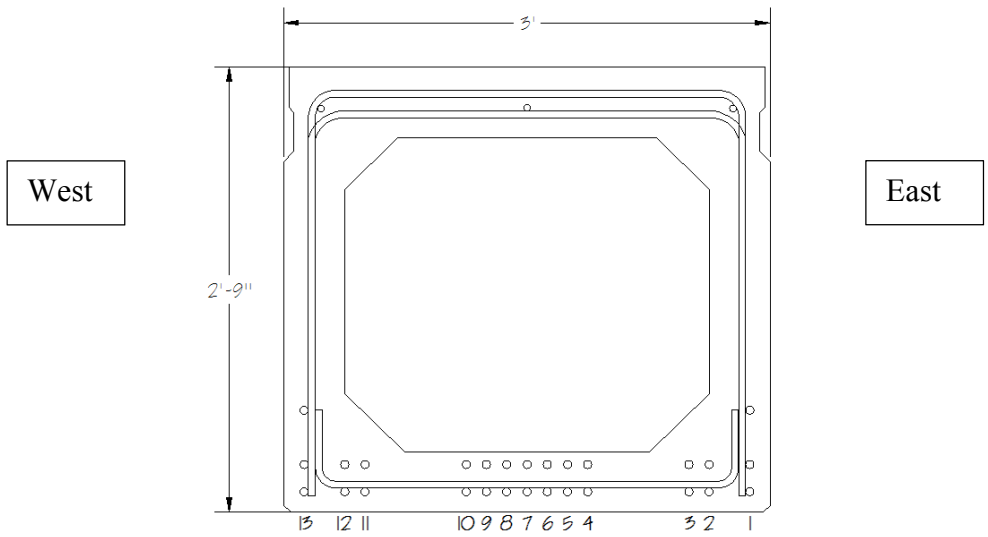

Figure 7: Typical Cross-section of Box Beams for US-24
Showing designated bar numbering and Overall Orientation.

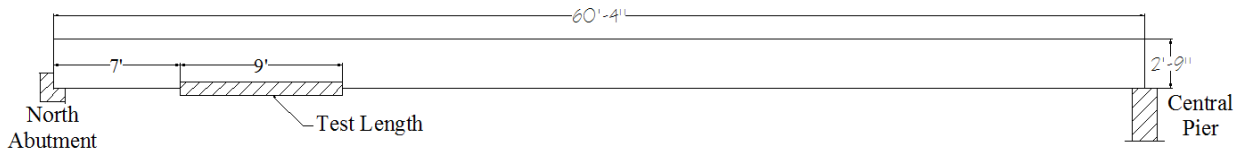

Figure 8: Longitudinal Section of Test Beams Showing Test Length from North Abutment

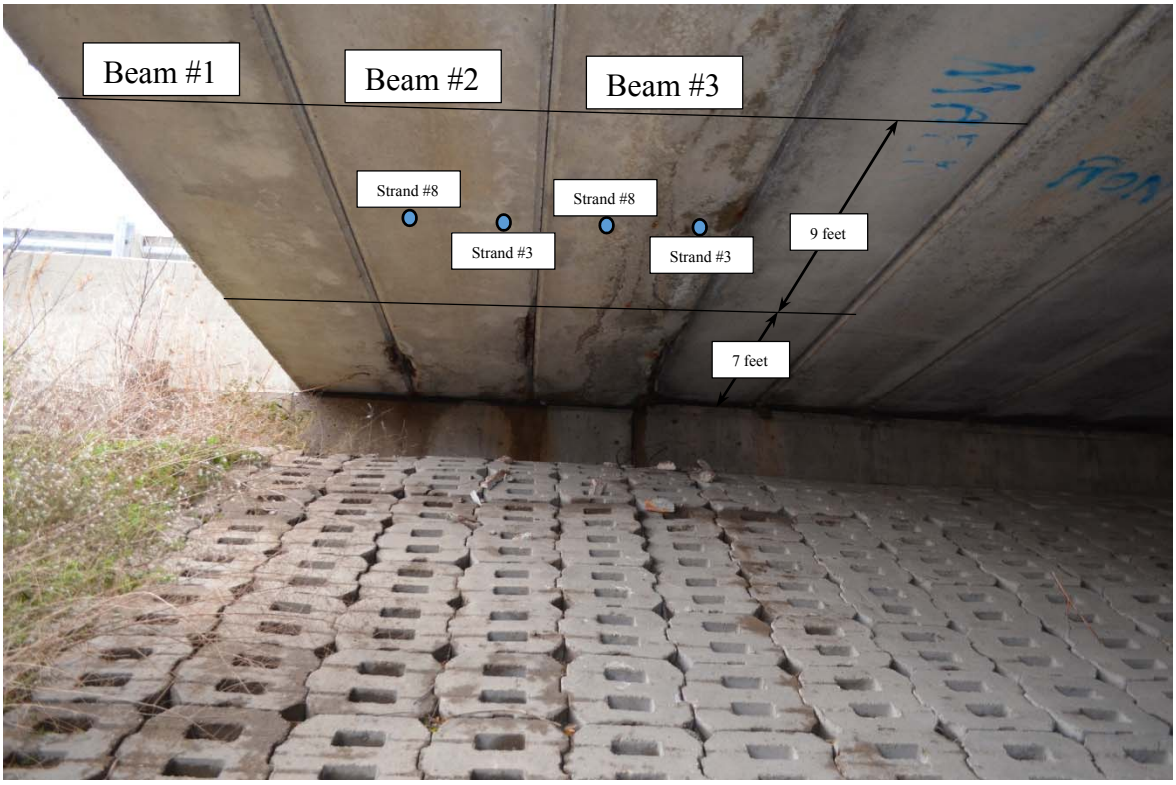

Figure 9: Designation of Scan Area and Location of Strands 3 and 8 for Beams 2&3

A.3 Background - Magnetic Flux Leakage Assessment of Box Beams

When a magnetic yoke is passed over a magnetic material, like reinforcement steel, the magnetic field passing from the north to the south pole of the magnet is channeled through the steel. The density of this magnetic field remains constant if both the magnetic material volume and the distance from the yoke to the magnetic material are constant. The magnetic field creates an electrical current and the resulting voltage can be measured. The voltage is denoted the Hall Voltage and Hall Sensors are used to measure the Hall Voltage as shown in Figure 11. When a change occur in either the magnetic material volume or the distance between the yoke and the magnetic material; the Hall Voltage also changes. This phenomena is utilized in methods such as rebar locators. In this field investigation this phenomena is utilized to detect changes of magnetic prestressing strands. The term magnetic flux leakage refers to the condition where the magnetic material volume decreases resulting in an increased magnetic saturation of the remaining steel and hence the magnetic flux density lines 'leak'. This phenomena is depicted in Figure 10.

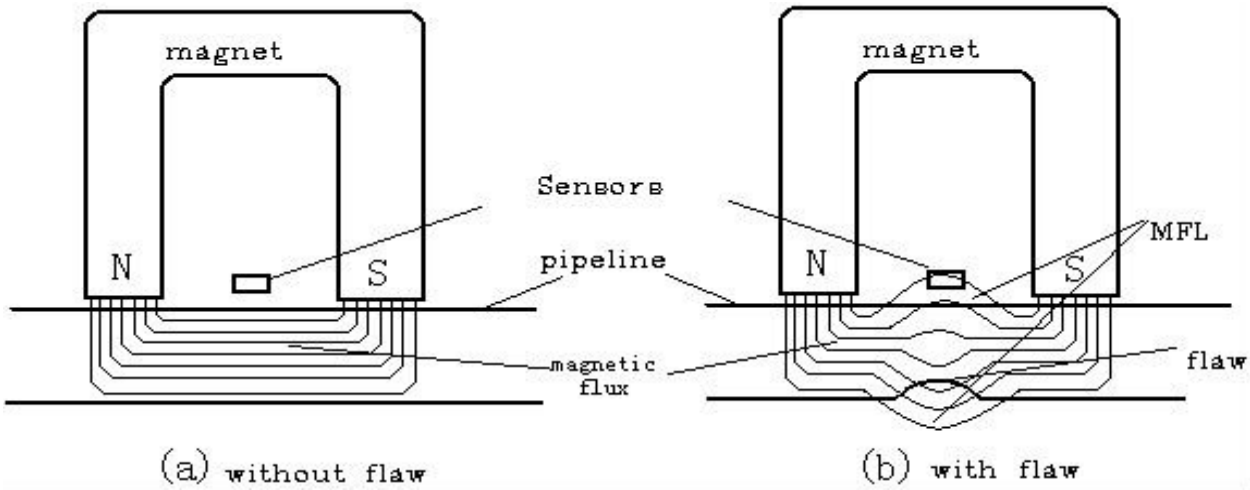

Figure 10. Depiction of magnetic flux density lines around magnetic member with or without cross sectional area reduction (ndt.net).

The Magnetic Flux Leakage system used in this study was developed at Lawrence Technological University. The strong earth magnet is mounted on a non-magnetic plate. Two sets of wheels and axles are mounted on the plate. Data is collected as the magnetic flux leakage (MFL) vehicle is passing along the concrete surface. The MFL equipment used on the bottom surface of the side-by-side ox beam bridge is shown in Figure 11.

Figure 11: MFL scanning set-up of box beams

Hall Voltage is collected from ten Hall Effect sensors, the distance traversed is measured by a rotary encoder, and the data acquisition system time stamps the data. Data are collected and stored approximately every 1 to 2 inches. An example of the variation of hall voltage as it passes over an area of cross sectional loss is shown in Figure 12. Two sets of data are shown in Figure 12 for a vertical and a horizontal placed hall sensor. Since the effect of concrete on magnetic field is negligible, the field leakage may be detected by sensors in the air near the surface of the concrete. If the magnetic source and sensors are moved along the length of the concrete member, the changes in the field, due to the presence of flaws in steel, can be recorded as continuous in terms of time and the field amplitude. This is then analyzed to obtain information relevant to the location and extent of the flaw in the steel (Ghorbanpoor, 1999).

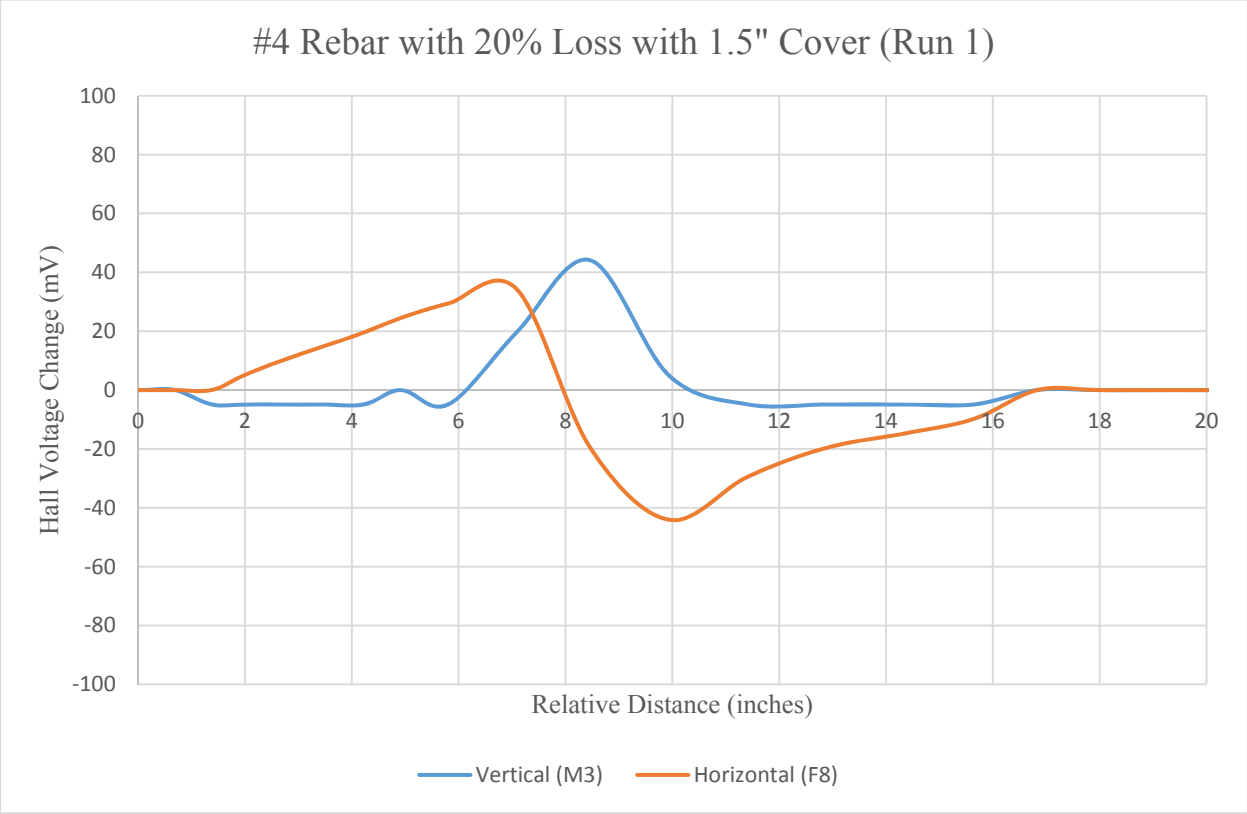

Figure 12. Variation in hall voltage output for area with or without cross sectional area reduction.

The system was calibrated using laboratory reinforced concrete beams as well as rebar. The variables considered were rebar size, rebar depth, localized loss of rebar material, and localized loss of strand material. For more details refer to section 3 of the main report. The relationship

between Hall Voltage and rebar cross sectional area for a rebar depth of 1.5 inches is shown in Figure 13 representing the vertical sensor (M3) in Figure 12. The rebar depth is the distance from the concrete surface to the center of the rebar. The relationship exhibits a stronger R^2 value for the parabolic than the linear relationship. The cross sectional area loss is predicted for this US-24 prestressed box beams bridge by using the relationship between Hall Voltage (*V*) and cross section area ($inch^2$), and regression parameters *a*, *b* and *c*:

$$y = ax^2 + bx + c \qquad \text{(Eq. 1)}$$

$$Hall\ Voltage\ (V) = 0.0263x^2 - 0.1976x + 2.9222$$

When estimating the cross sectional area considering the measured change in hall voltage the overall system offset given by parameter c is excluded from the calculations.

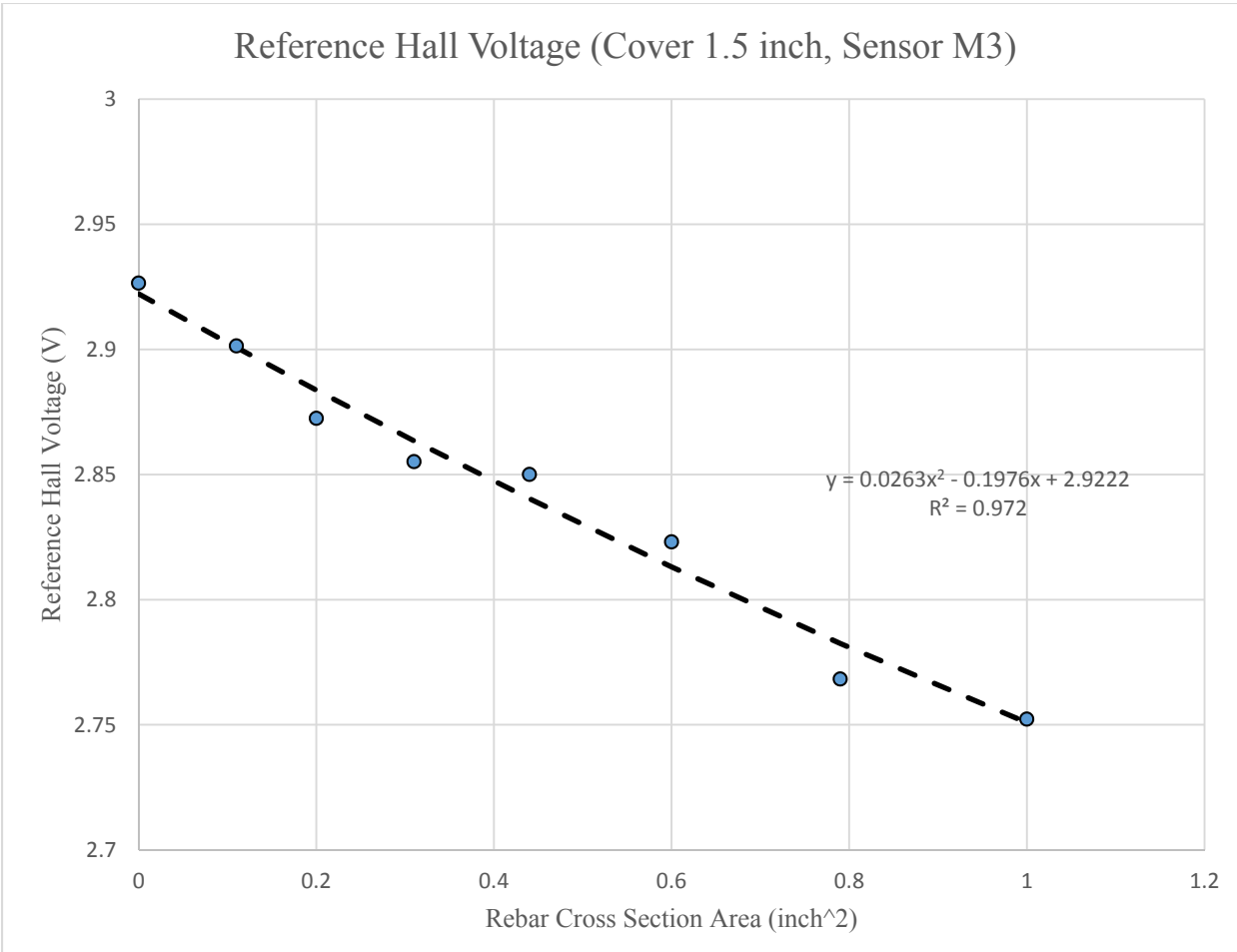

Figure 13. Relationship between hall voltage and cross sectional area of rebar for concrete cover of 1.5 inches.

The relationships between predicted and actual cross sectional area loss over a 12 inch length of a rebar are shown in Figure 14 for steel stirrup spacing of 9.5 and 19 inches, respectively. In both cases the rebar depth is 1.5 inches. There is excellent agreement between predicted and actual cross sectional area loss for Beam 2 with stirrup spacing of 9.5 inches. There is adequate agreement for the case of stirrup spacing of 19 inches. The slopes of the linear prediction curves are very similar ranging from 0.78 to 0.82. The offset is, however, different between the two sets of data with 4% and 16% overestimation at 0% loss, respectively.

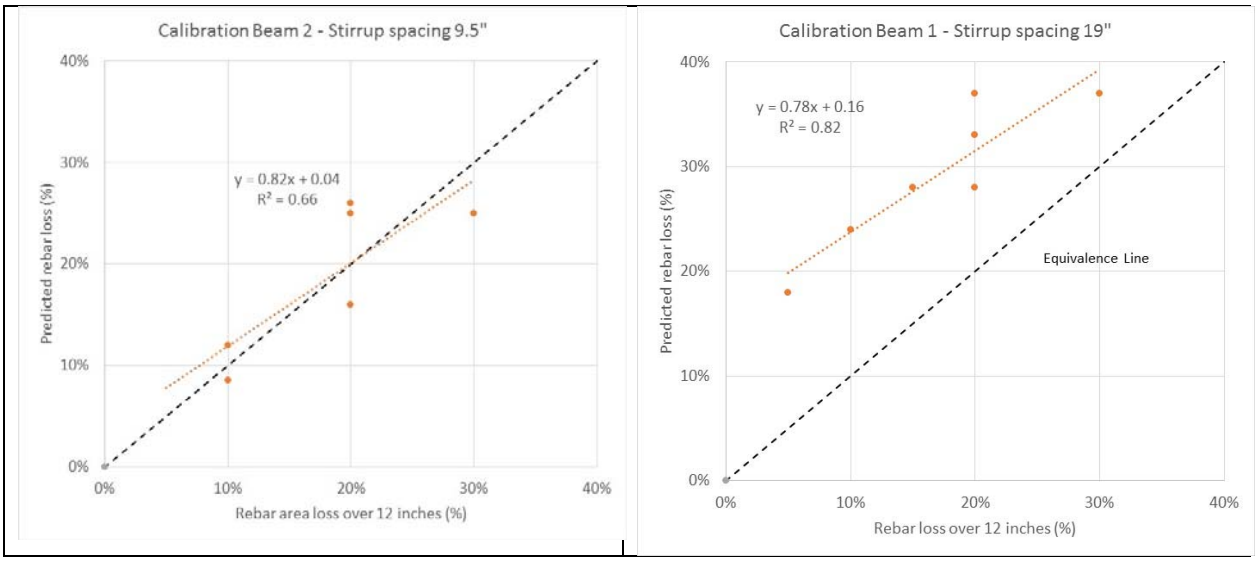

Figure 14. Predicted rebar cross sectional area loss versus actual rebar cross sectional area loss over 12 inches in calibration beams.

A.4 Magnetic Flux Leakage Assessment of Prestressing Strands

Each assessable strand along the selected segment was scanned three times. In each case the measurements were taken south to north (from mid span area towards the northern abutment as shown in Figure 8). The effective scan length varies as surface spalling may have rendered the reference surface uneven. The use of MFL system overhead is shown in Figure 11.

The relative variation of the hall voltage along the length of the testing area is shown in Figure 15 and Figure 16 for Box Beam 2, Strand 8 and Box Beam 3, Strand 4 respectively. Consider the stirrup locations along the testing length to be aligned as shown with the vertical lines. There is a slight variation of the relative hall voltage for Box Beam 2, Strand 8 indicating insignificant change in magnetic material. Furthermore, the three runs are in fairly good agreement. On the other hand, Box Beam 3, Strand 4 exhibit significant variation of the relative hall voltage on the other of 25 to 30 mV. A relative high value (positive) indicates reduced magnetic material. Strand 4 therefore shows reduced cross section area in several areas. Applying equation 1 yields a predicted loss of cross section area of up to 90 to 100%. Taking the estimated over prediction into account the loss is estimated in areas to be as high as 75%. Furthermore, it is important to recall that the 3/8", 7 wire strand's cross section area is 0.085 in^2 and on the lower boundary covered in the laboratory calibration.

In some instances the readings were erroneous or the concrete surface reference was lost due to spalling. The data in Figure 17 illustrates such a case for Box Beam 3, Strand 3. The three runs are consistent up to 20 inches after which the data deviates. After this point spalling and visual strand corrosion hinders data collection. Strand 1 and Strand 2 in Box Beam 3 are corroded and broken.

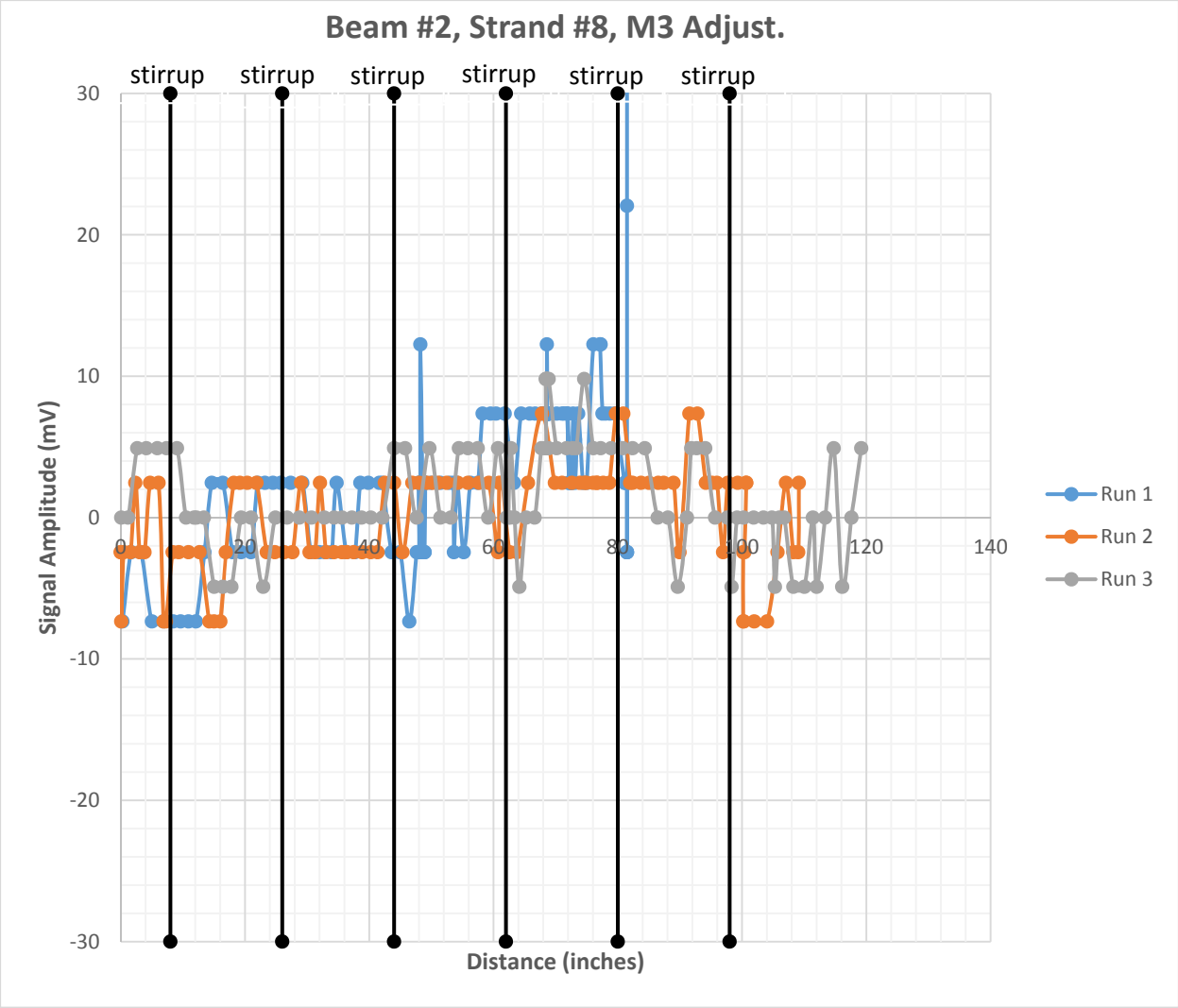

Figure. 15: Relative Hall voltage along testing length (south towards north) for Box Beam 2 Strand 8

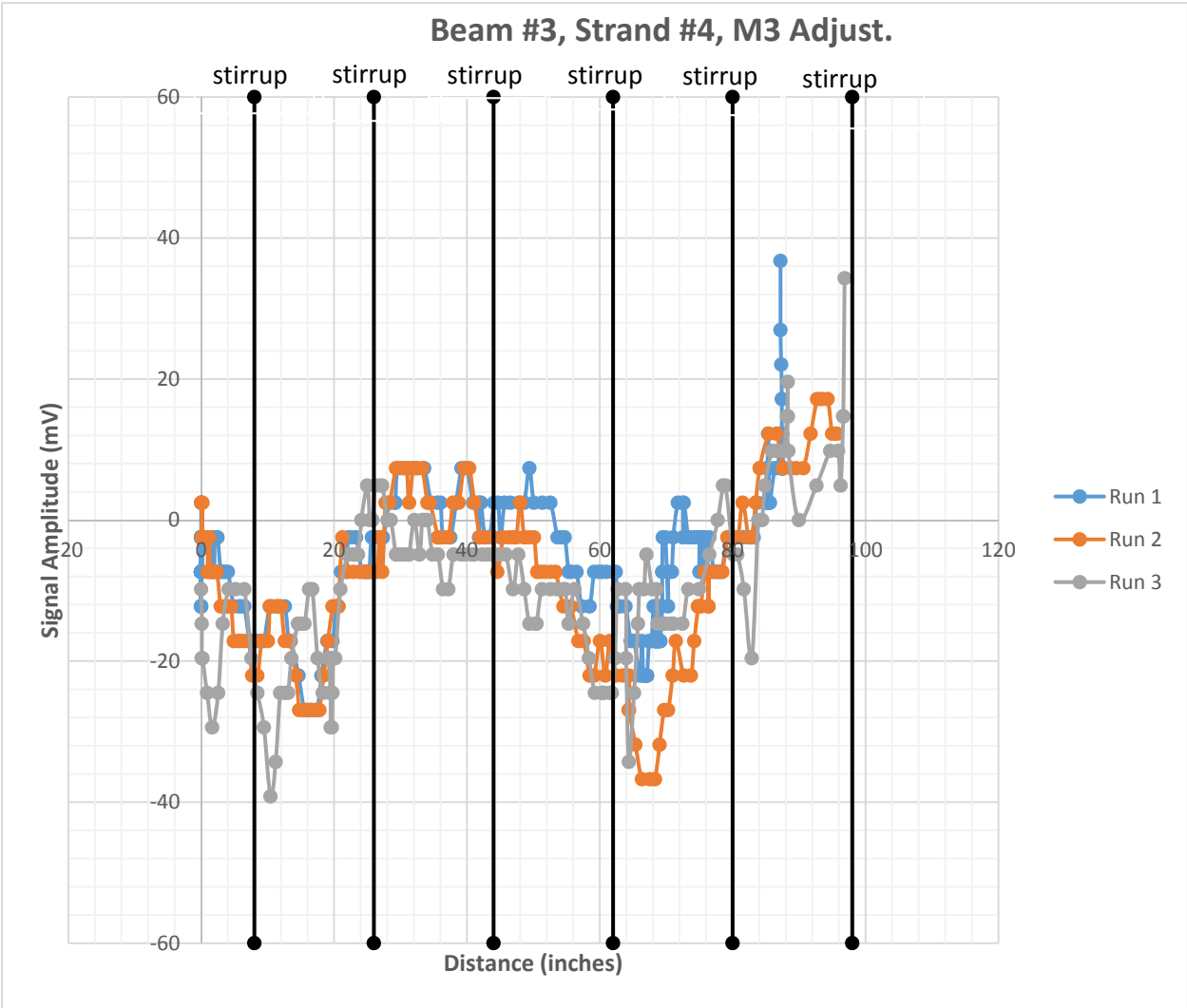

Figure. 16: Relative Hall voltage along testing length (south towards north) for Box Beam 3 Strand 4

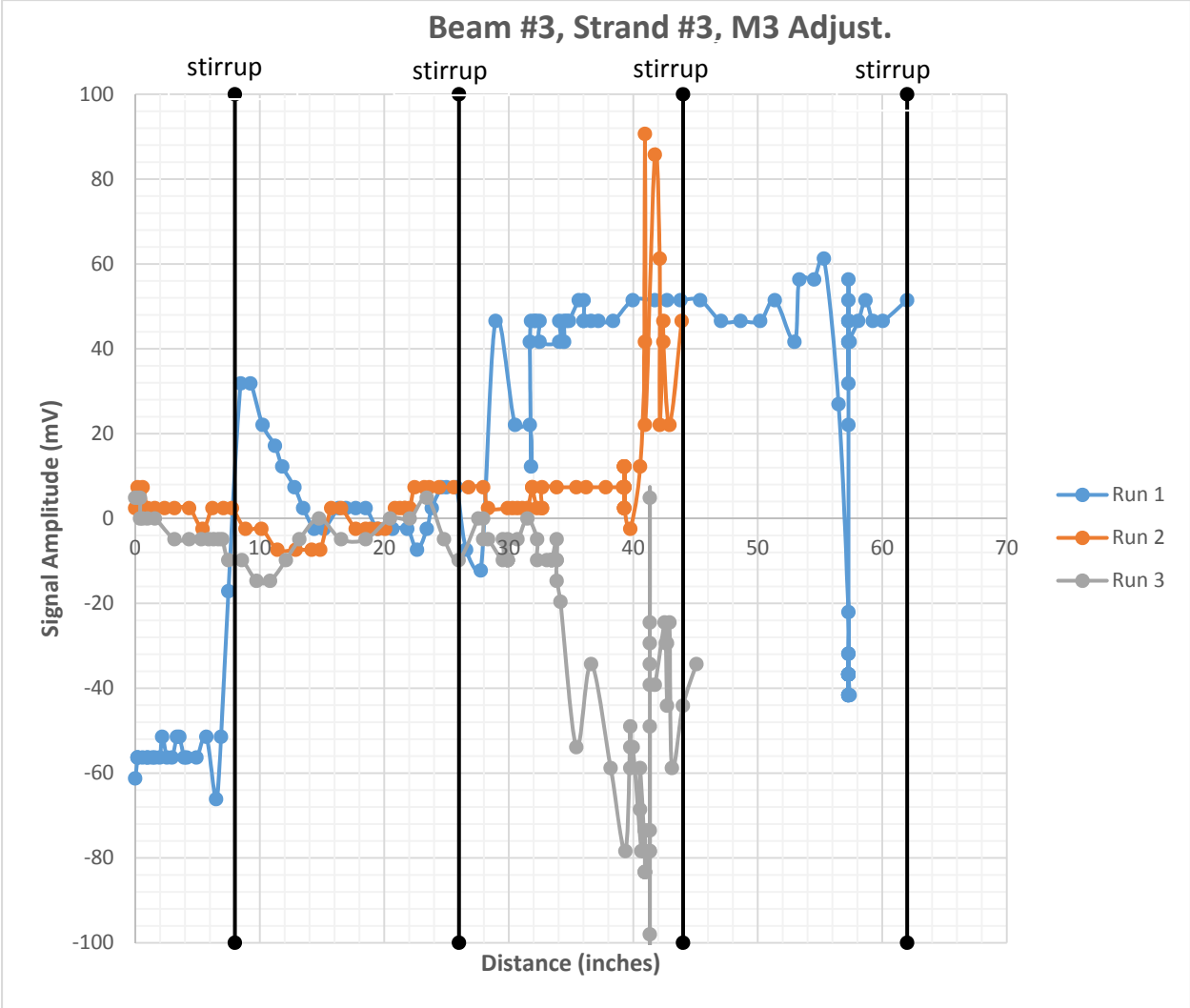

Figure. 17: Relative Hall voltage along testing length (south towards north) for Box Beam 3 Strand 3

Table 1 summarizes the estimated loss of cross section area considering the single strand in the bottom layer (Figure 7) of Box Beam #3. It is assumed that the strand in the second layer is not interfering with the relative variation of the Hall Voltage. This is a reasonable assumption as the depth of the second layer is 2 inches above the bottom layer.

It can be deduced from a combination of visual inspection and the detailed magnetic flux leakage assessment of Box Beams that, the beam maintains capacity due to double layer of prestressing as can be seen from Figure 9. The effect of transverse post-tensioning of adjacent box beams may also enhance the capacity due to the load distribution effect.

Table 1. Estimated Loss of Cross Section Area of 3/8 7 Wire Strand, Grade 270 in Beam 3, bottom layer. Noise Band ±5 mV. Reference Voltage 16.606 mV. The column 'Loss' is considering the overestimation.

Strand	Distance Start	Distance Stop	Offset	Change	Remaining Voltage	Remaining Area	Real Loss (up to)
#	in	in	mV	mV	mV	in^2	%
1	0	120					Broken
2	0	120					Broken
3	0	30	5	0	16.61	0.085	0
3	30	120					NOISE or ERROR
4	20	50	5	0	16.61	0.085	0
4	20	50	20	15	1.61	0.008	75
4	60	80	20	15	1.61	0.008	75
4	80	100	25	20	-3.39	-0.017	100
5	0	20	5	0	16.61	0.085	0
5	20	45	20	15	1.61	0.008	75
5	45	62	10	5	11.61	0.060	15
5	62	90	20	15	1.61	0.008	75
6	0	25	5	0	16.61	0.085	0
6	25	50	20	15	1.61	0.008	75
6	50	80	5	0	0.00	0.00	85
6	80	100	25	20	-3.39	-0.017	100
7	20	65	15	10	6.61	0.034	45
8	0	25	5	0	16.61	0.085	0
8	25	50	15	10	6.61	0.034	45
8	70	90	15	10	6.61	0.034	45
9	0	25	5	0	16.61	0.085	0
9	25	42	10	5	11.61	0.060	15
9	42	108	5	0	16.61	0.085	0

10	0	108					NOISE or ERROR
11	0	108					NOISE or ERROR
12	0	108	5	0	16.61	0.085	0
13	0	109					NOISE or ERROR

Box Beam #2 shows some variation in the Hall Voltage readings for the edge strands 1, 2 and 3. However, it shows at best some beginning disturbances and that is interpreted in this study as beginning corrosion of the strands. Due to the small cross section size of the 3/8" 7 wire strand the corrosion is likely on the order of 10-15% in these strands (considered laboratory calibration data). See Figure 18.

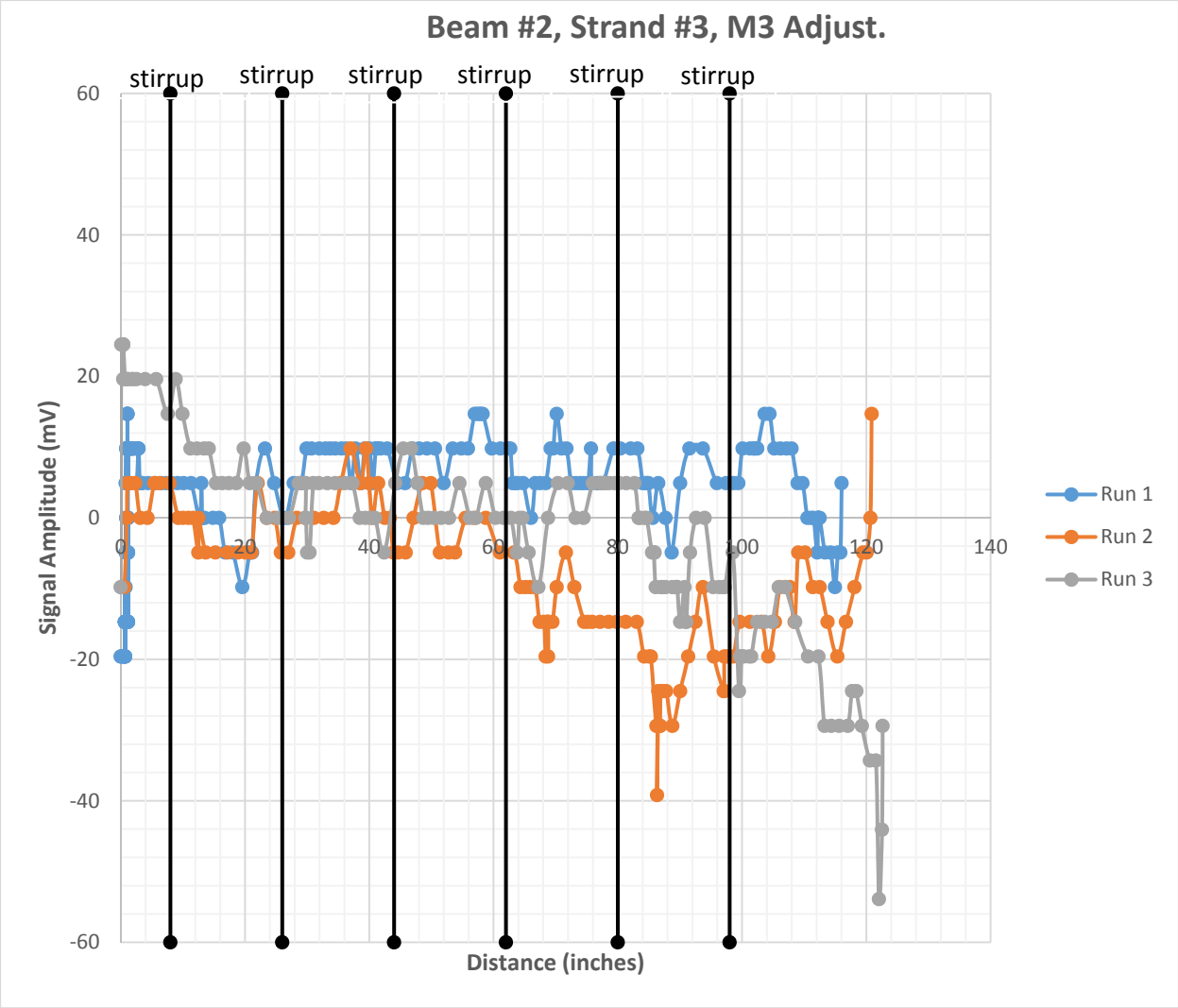

Figure. 18: Relative Hall voltage along testing length (south towards north) for Box Beam 2 Strand 3

A.5 Ultrasonic Assessment of Box Beams

Ultrasonic testing uses high frequency sound energy to excite the concrete material. Ultrasonic inspection can be used for flaw detection/evaluation, dimensional measurements, material characterization, and more. Ultrasonic waves are mechanical waves with frequencies normally higher than 20 kHz that propagate through concrete material. Condition and properties of the test material are determined by analyzing various properties of the sent and received waves. Ultrasonic assessment was not used to directly detect corrosion of embedded strands, but instead to detect typical deterioration of concrete such as delamination, cracking and spallings that is associated with the corrosion process.

A typical ultrasonic inspection system consists of several functional units, such as the pulser/receiver, transducer, and display devices. A pulser/receiver is an electronic device that can produce high frequency electrical pulses. Driven by the pulser, the transducer generates high frequency ultrasonic energy. The sound energy is introduced and propagates through the materials in the form of waves. When there is a discontinuity (such as a crack) in the wave path, part of the energy will be reflected back from the flaw surface. The reflected wave signal is transformed into an electrical signal by the transducer and is displayed often on a screen. Signal travel time can be directly related to the distance that the signal traveled. From the signal, information about the reflector location, size, orientation and other features may be gained.

Ultrasonic assessment using MIRA was conducted along the bottom strands to complement the results of the MFL assessment. The assessment was conducted mainly to check for the extent of delamination and the presence of voids along the corroded strands using scanning frequencies 50 kHz, 80 kHz and 100 kHz. Each strand was scanned 3 times at each selected frequency to aid in the analysis of the scanned results. Details of box beams were extracted from as-built drawings with designation Brighton-Detroit Road from Job Number 01247A DWG No. B03 of 82053C, Superstructure Details. Figure 19 shows a typical ultrasonic scanning set-up of the box beams using MIRA.

Fig. 19: Ultrasonic scanning set-up for box beams.

A side-by-side comparison of scans at a frequency of 80 kHz and 40 decibel (dB) on strands with visible signs of corrosion as against strands without visible signs of corrosion showed there were significant differences in scans intensity. Details have been shown below for Figure 20 (a) (b) (c) & (d) showing scans from strands with visible signs of corrosion and Figure 21 (a) (b) (c) & (d) showing scans from strands without visible signs of significant corrosion. Detailed comparison of the two sets of scans clearly show that due to significant voids around strands in the case of Figure 20, the intensity of the reflections are higher compared to those of Figure 21. This is because the ultrasonic assessment is based on the principle that, intensity of reflections are related to the magnitude of the change in material properties such as density and elastic modulus as shear waves propagates through the concrete materials which are normally associated with delamination, spallings as well as cracking of concrete.

The rule of thumb for detecting delamination, cracking, spallings and other discontinuities is that, the size of the discontinuity must be greater than half of the scanning wave length to stand a reasonable chance of being detected. Using the relation: $\lambda = \frac{v}{f}$ where λ = wave length, v = velocity and f = frequency. Considering the selected scanning frequencies of 50, 80 and 100 kHz and considering a good concrete with an average shear wave velocity of 2500 ms^{-1}, a defect size should be greater than half of the wavelengths which are within the range of 25 mm for 50 kHz and 12.55 mm for 100 kHz to stand a reasonable chance of being detected.

The following colour codes have been selected for presentation.

no change in shear wave reflection

medium change in shear wave reflection

high change in shear wave reflection

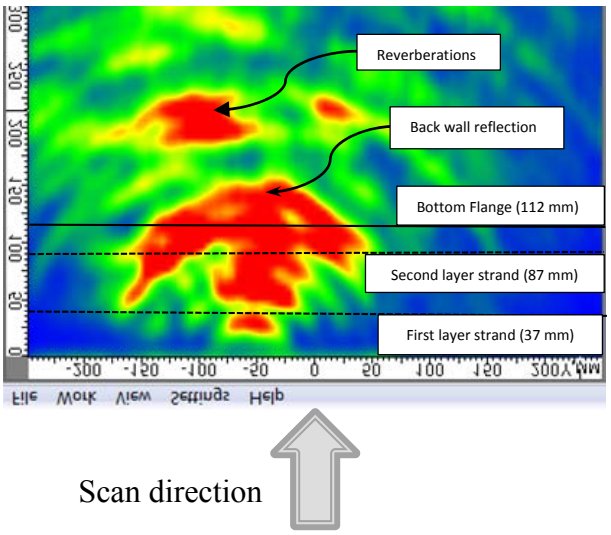

Figure 20 (a): Beam 3, strand #3, 80 kHz

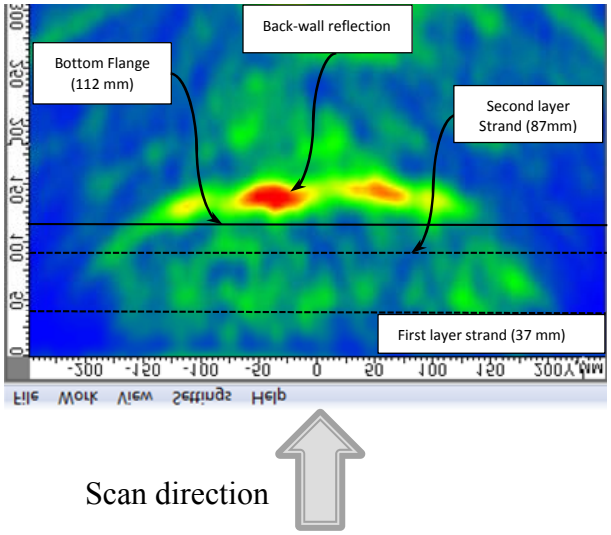

Figure 21 (a): Beam 2, strand 3, 80 kHz

Center of scan is 9'-7.5" (2890 mm) from face of North Abutment

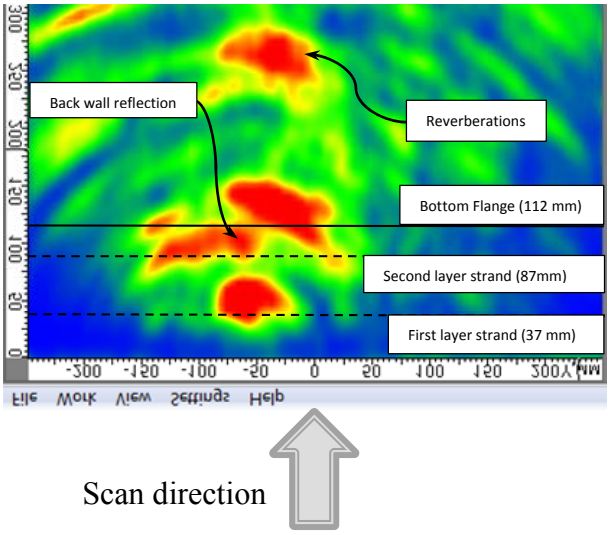

Figure 20 (b): Beam 3, strand #3, 80 kHz

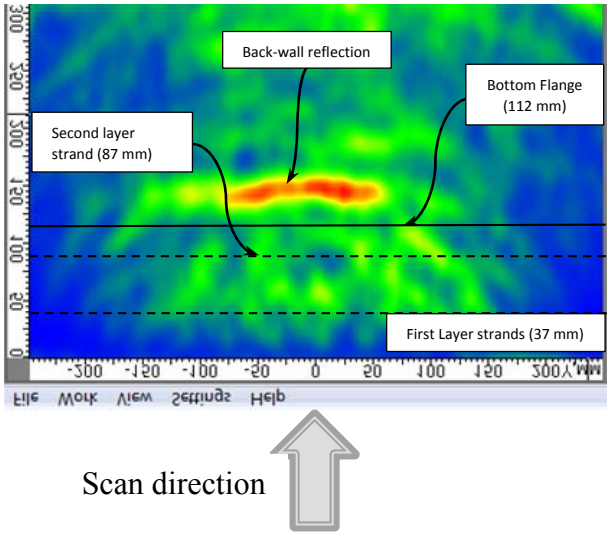

Figure 21 (b): Beam 2, strand 3, 80 kHz

Center of scan is 8'-2.4" (2460 mm) from face of North Abutment

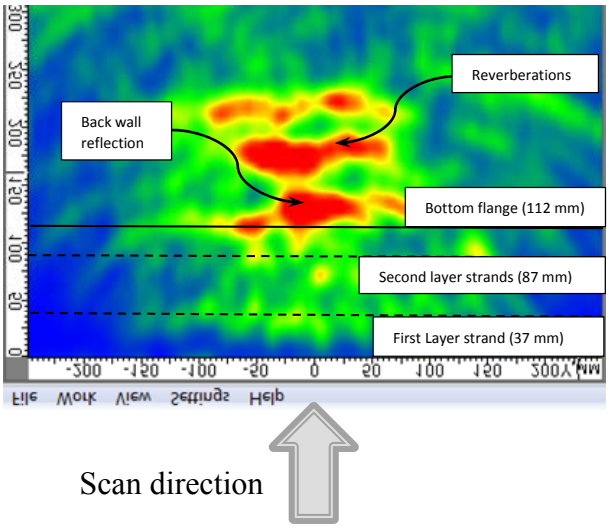

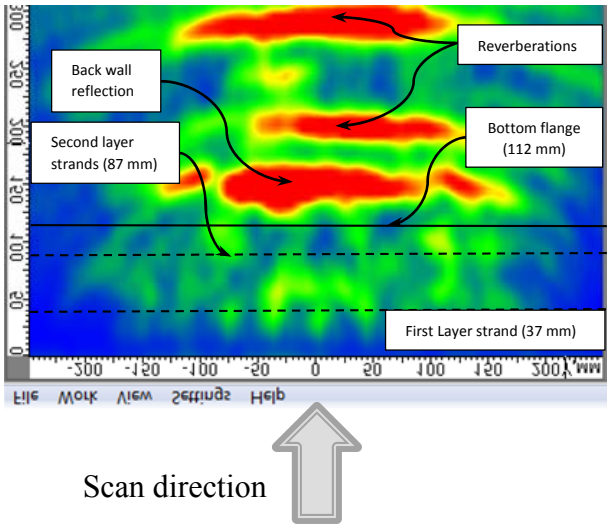

Figure 20 (c): Beam 3, strand #8, 80 kHz *Figure 21 (c): Beam 2, strand 8, 80 kHz*

Center of scan is 13'-10.2" (4160 mm) from face of North Abutment

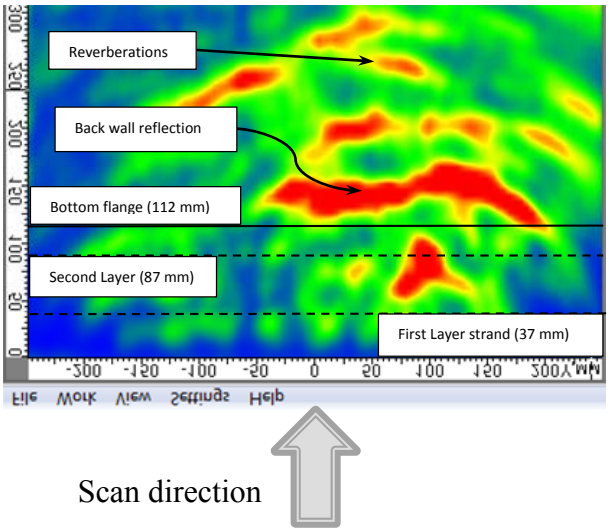

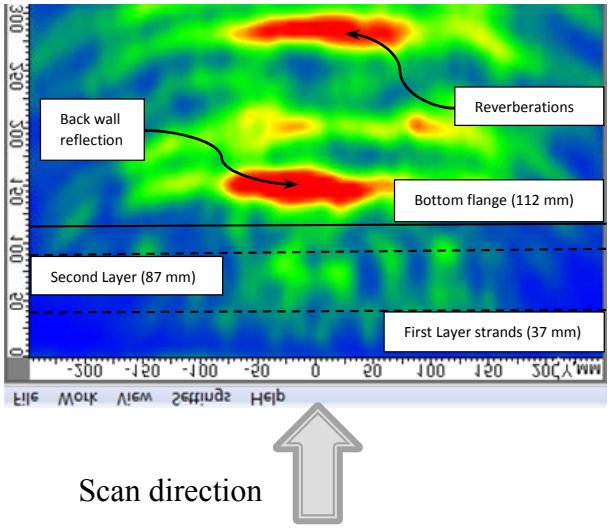

Figure 20 (d): Beam 3, strand #8, 80 kHz *Figure 21 (d): Beam 2, strand 8, 80 kHz*

Center of scan is 12'-5.5" (3740 mm) from face of North Abutment

APPENDIX B

IMPLEMENTATION PLAN

Department of Civil and Architectural Engineering

Lawrence Technological University

Southfield, MI 48075-0134

November 2015

B.1 General

Based on the results presented in the main report, an implementation plan is proposed to employ ultrasonic echo-pulse tomography and electrochemical hall-cell potential difference measurements to evaluate the condition of bridges exhibiting deterioration associated with corrosion of the steel reinforcement. These two methods are well established, field worthy, and their equipment are commercially available. The study also evaluated the use of the magnetic flux leakage method to detect and quantify corrosion of the steel reinforcement. The method is very promising, however, there are no readily available commercially units at the time of this study. The application of these three methods are summarized in Table 1. In general, ultrasonic assessment is recommended to assess delamination, debonding of reinforcement due to corrosion, and void detection. Electrochemical half-cell potential assessment is recommended to identify areas in the structure experiencing increased chance of corrosion. The recommendations set forth are specific to the nondestructive test methods evaluated in this study. Please consult the literature on the application and recommended use of other methods such as ground penetrating radar, infrared thermography, acoustic sounding, and others.

Table 1: Selection Matrix to Detect and Quantify Defects

Component	Defects	NDE Methods to Detect	NDE methods to Quantify
Reinforcement	Delamination & Voids	Ultrasonic	Ultrasonic
	Corrosion Activity	Hall-cell	-
	Loss of X-section Area	*MFL	*MFL
PT Ducts	Voids/Grout Issues	Ultrasonic	Ultrasonic

*MFL – not yet field worthy

Ultrasonic testing was performed with MIRA, a 3D ultrasonic echo-pulse tomographer, using shear waves low-frequency phased antenna arrays. The corrosion half-cell potential difference measurements were completed using a copper-copper sulfate reference electrode. The equipment used is known as CANIN.

B.2. Ultrasonic Tomography

Ultrasonic assessment can detect deterioration of concrete such as debonding, delamination, and cracking that follows the corrosion process. Therefore, ultrasonic assessment can be employed as an indirect tool to detect corrosion of strands and reinforcement embedded in concrete. The ultrasonic pulse-echo equipment, used in this study, coalesces the data responses from forty individual transducers that act as both transmitters and receivers. The transducers are arranged in an array with 4 rows and 10 columns covering a 4 in by 16 in (100 mm by 400 mm) surface area.

B.2.1 Data Collection Recommendations

- When evaluating the deterioration along the reinforcement it is recommended that the equipment be aligned and traversing with its longitudinal axis directly centered on the concrete surface above the longitudinal direction of the reinforcement.
- When evaluating the grouting uniformity in post-tensioned ducts it is recommended that the equipment be aligned and traversing with its transverse axis directly centered on the expected longitudinal direction of the duct.
- Testing should be carried out over large areas on the surface of structure to aid in detecting deviations from normal reflections. The intensity of reflections were always higher in areas with defects around the steel reinforcement than in areas without defects.
- The assessment over large areas of the structure will serve as a self-calibration since factors related to operator, materials, and construction can be assumed to impact the measurements equally.
- When evaluating the conditions around reinforcement located 1.5 to 2.0 inches (37 to 50 mm) below the surface, three different scan frequencies should be used ranging from 50 to 70 kHz. Application of higher frequencies should be avoided when assessing near surface features or thin structures such as box beam web or flanges.
- When evaluating the grout condition in post-tensioned ducts located 3 or more inches below the surface, one scan frequency of about 50 kHz can be used.
- Three repeated sets of data should be collected at each scan frequency and it is recommended to lay out a test grid on the concrete surface, prior to data collection.

- It is recommended that ultrasonic condition assessment is supported by a second method that is based on another nondestructive testing method such as electrochemical and ground penetrating radar.

B.2.2. Data Collection Issues

- The 3D images of the ultrasonic reflections allow the data analyst to determine the location and depth of the defect. However, the horizontal length of the defect is not quantified.
- In advanced cases of corrosion with extensive delamination and cracking around the reinforcement, ultrasonic reflections near the corroded strands and reinforcement tend to produce voluminous surface noise and other multiple reflections. These reflections tend to mask the actual reflections near the strands and any back-wall reflection from features such as the interior cell in a box beam.
- Similarly, data obtained when using high scan frequencies, such as 80 kHz and above, tend to produce voluminous surface noise and other multiple reflections. These data may be ambiguous. Care should be taken during testing and analysis with the adjustment of the measuring frequency to reduce the amount of attenuation.
- Care should be taken when collecting data on the most outer reinforcement strand located at the longitudinal edge, along the shear key, in box beams. It must be verified that all tomographer sensors are placed on the same plane surface. It may be necessary to discard data if this condition is not satisfied.
- It is recommended that the operator and the data analyst is familiar with the structure prior to testing. Information such as plan sheets, bridge inspection data, and any maintenance records should be made available and reviewed.
- Operators and data analysts should be trained prior to use of the equipment. It is recommended that dummy specimens with known defects are used as part of the training.
- The 3D ultrasonic echo-pulse tomographer is a handheld device that can be used on horizontal (incl. overhead) and vertical concrete surfaces. Care should be taken to ensure that all the sensors are in full contact with the concrete surface when used overhead.

B.3. Electrochemical Half-cell Potential

The study also recommends the use of electrochemical assessment as part of monitoring the change in the chance of corrosion of the reinforcement in areas that exhibit surface cracking developed during construction, early deterioration, or other factors. The field application and data analysis should be conducted according ASTM C876 - 09 Standard Test Method for Corrosion Potentials of Uncoated Reinforcing Steel in Concrete.

B.3.1 Data Collection Recommendations

- Testing should be carried out over large areas of the structure's surface to aid in detecting deviations from normal values of half-cell potential differences.
- Condition assessment over large areas of the structure will serve as a self-calibration since factors related to operator, materials, and construction can be assumed to impact the measurements equally.
- It is recommended to use both contour plots and frequency plots during data analysis. Contour plots quickly identifies regions with significant change in potentials and the frequency plots quickly illustrates the relative area with high, medium and low chance of corrosion.
- It is recommended that electrochemical condition assessment is supported by a second method that is based on another nondestructive testing method such as ultrasound and ground penetrating radar.

B.3.2. Data Collection Issues

- Additional data analysis and calibration may be necessary when existing cracks have been sealed with a non-cementitious material.
- Concrete surface areas with highly varying porosity due to poor consolidation may give ambiguous results.
- Care should be exercised when taking measurements overhead that the sensor is in full contact with the concrete surface.